Beyond Local Nash Equilibria for Adversarial Networks*

Frans A. Oliehoek Rahul Savani Jose Gallego Elise van der Pol Roderich Groß

July 17, 2022

Abstract

Save for some special cases, current training methods for Generative Adversarial Networks (GANs) are at best guaranteed to converge to a 'local Nash equilibrium' (LNE). Such LNEs, however, can be arbitrarily far from an actual Nash equilibrium (NE), which implies that there are no guarantees on the quality of the found generator or classifier. This paper proposes to model GANs explicitly as finite games in mixed strategies, thereby ensuring that every LNE is an NE. With this formulation, we propose a solution method that is proven to monotonically converge to a resourcebounded Nash equilibrium (RB-NE): by increasing computational resources we can find better solutions. We empirically demonstrate that our method is less prone to typical GAN problems such as mode collapse, and produces solutions that are less exploitable than those produced by GANs and MGANs, and closely resemble theoretical predictions about NEs.

1. Introduction

Generative Adversarial Networks (GANs) (Goodfellow et al., 2014) are a framework in which two neural networks compete with each other: the *generator* (*G*) tries to trick the *classifier* (*C*) into classifying its generated fake data as true. GANs hold great promise for the development of accurate generative models for complex distributions. Consequently, in just a few years, GANs have grown into a major topic of research in machine learning. A core appeal is that they do not need to rely on distance metrics (Li et al., 2016). However, GANs are difficult to train (Unterthiner et al., 2018; Arjovsky and Bottou, 2017; Arjovsky et al., 2017). A typical problem is *mode collapse*, which can take the form of *mode omission*, where the generator does not produce points from certain modes, or *mode degeneration*,

in which for at least one mode the generator only partially covers the mode. Moreover, while learning the players may forget: e.g., it is possible that a classifier correctly learns to classify part of the input space as 'fake' only to forget this later when the generator no longer generates examples in this part of space. In fact, except for very special cases (cf. Section 7), the best current training methods can offer (Heusel et al., 2017; Unterthiner et al., 2018) is a guarantee to converge to a *local* Nash equilibrium (LNE) (Ratliff et al., 2013). However, an LNE can be arbitrarily far from an NE (which we will also refer to as 'global NE' to discriminate) and the corresponding generator might be exploitable by a strong opponent due to suffering from problems such as mode collapse. Moreover, adding computational resources alone may not offer a way to escape these local equilibria: the problem does not lie in the lack of computational resources, but is inherently the result of only allowing small steps in strategy space using gradient-based training.

We introduce a novel approach that does not suffer from getting trapped in LNEs: finite *Generative Adversarial Network Games (GANGs)* formulate adversarial networks as *finite* zero-sum games, and the solutions that we try to find are saddle points in *mixed strategies*. This approach is motivated by the observation that, considering a GAN as a finite zero-sum game, in the space of mixed strategies, any local Nash equilibrium is a global one. Intuitively, the reason for this is that whenever there is a profitable pure strategy deviation one can move towards it in the space of mixed strategies.

Since we cannot expect to find exact best responses due to the extremely large number of pure strategies that result for sensible choices of neural network classes, we introduce resource-bounded best-responses (RBBRs), and the corresponding resource-bounded Nash equilibrium (RB-NE), which is a pair of mixed strategies in which no player can find a better RBBR. This is richer than the notion of local Nash equilibrium in that it captures not only failures of escaping local optima of gradient descent, but applies to *any* approximate best response computations, including methods with random restarts, and allows us to provide convergence guarantees.

^{*}This version supersedes our earlier arXiv paper (Oliehoek et al., 2017).

The key features of our approach are that:

- It is based on finite zero-sum games, and as such it enables
 the use of existing game-theoretic methods. In this paper
 we focus on one such method, Parallel Nash Memory
 (PNM) (Oliehoek et al., 2006).
- It will not get trapped in LNEs: we prove that it monotonically converges to an RB-NE, which means that more computation can improve solution quality.
- Moreover, it works for any network architecture (unlike previous approaches, see Section 7). In particular, future improvements in classifiers/generator networks can be exploited directly.

We investigate empirically the effectiveness of PNM and show that it can indeed deal well with typical GAN problems such as mode collapse and forgetting, especially in distributions with asymmetric structure to their modes. We show that the found solutions are much less susceptible to being exploited by an adversary, and that they more closely match the theoretical predictions made by Goodfellow et al. (2014) about the conditions at a Nash equilibrium.

2. Background

We defer a more detailed treatment of related work on GANs and recent game-theoretic approaches until Section 7. Here, we introduce some basic game-theoretic notation.

Definition 1 ('game'). A two-player strategic game, which we will simply call 'game', is a tuple $\langle \mathcal{D}, \{\mathcal{S}_i\}_{i\in\mathcal{D}}, \{u_i\}_{i\in\mathcal{D}} \rangle$, where $\mathcal{D} = \{1,2\}$ is the set of players, \mathcal{S}_i is the set of pure strategies (actions) for player i, and $u_i: \mathcal{S} \to \mathbb{R}$ is i's payoff function defined on the set of pure strategy profiles $\mathcal{S} := \mathcal{S}_1 \times \mathcal{S}_2$. When the action sets are finite, the game is finite.

We also write s_i and s_{-i} for the strategy of agent i and its opponent respectively.

A fundamental concept is the Nash equilibrium (NE), which is a strategy profile such that no player can unilaterally deviate and improve his payoff.

Definition 2 (Pure Nash equilibrium). A pure strategy profile $s = \langle s_i, s_{-i} \rangle$ is an NE if and only if $u_i(s) \geq u_i(\langle s'_i, s_{-i} \rangle)$ for all players i and $s'_i \in \mathcal{S}_i$.

A finite game may not possess a pure NE. A *mixed strategy* μ_i of player i is a probability distribution over i's pure strategies \mathcal{S}_i . The set of such probability distributions is denoted by $\Delta(\mathcal{S}_i)$. The payoff of a player under a profile of mixed strategies $\mu = \langle \mu_1, \mu_2 \rangle$ is defined as the expectation: $u_i(\mu) := \sum_{s \in \mathcal{S}} [\prod_{j \in \mathcal{D}} \mu_j(s_j)] \cdot u_i(s)$.

Then an NE in mixed strategies is defined as follows.

Definition 3 (Mixed Nash equilibrium). A $\mu = \langle \mu_i, \mu_{-i} \rangle$

is an NE if and only if $u_i(\mu) \ge u_i(\langle s_i', \mu_{-i} \rangle)$ for all players i and potential unilateral deviations $s_i' \in \mathcal{S}_i$.

Every finite game has at least one NE in mixed strategies (Nash, 1950). In this paper we deal with two-player zero-sum games, where $u_1(s_1, s_2) = -u_2(s_1, s_2)$ for all $s_1 \in \mathcal{S}_1, s_2 \in \mathcal{S}_2$. The equilibria of zero-sum games, also called saddle points, have several important properties, as stated in the Minmax theorem.

Theorem 1 (von Neumann (1928)). In a finite zero-sum game, $\min_{\mu_2} \max_{\mu_1} u_1(\mu) = \max_{\mu_1} \min_{\mu_2} u_1(\mu) = v^*$, where v^* is the value of the game.

All equilibria have payoff v^* and equilibrium strategies are interchangeable: if $\langle \mu_1, \mu_2 \rangle$ and $\langle \mu_1', \mu_2' \rangle$ are equilibria, then so are $\langle \mu_1', \mu_2 \rangle$ and $\langle \mu_1, \mu_2' \rangle$ (Osborne and Rubinstein, 1994). This means that in zero-sum games we do not need to worry about equilibrium selection: any equilibrium strategy for a player is guaranteed to achieve the value of the game. Moreover, the convex combination of two equilibria is an equilibrium, meaning that the game has either one or infinitely many equilibria.

We also employ the standard, additive notion of *approximate* equilibrium:

Definition 4. A pair of (possibly pure) strategies (μ_i, μ_{-i}) is an ϵ -NE if $\forall i \quad u_i(\mu_i, \mu_{-i}) \geq \max_{\mu'_i} u_i(\mu'_i, \mu_{-i}) - \epsilon$. In other words, no player can gain more than ϵ by deviating.

In the literature, GANs have not typically been considered as finite games. The natural interpretation of the standard setup of GANs is of an infinite game where payoffs are defined over all possible weight parameters for the respective neural networks. With this view we do not obtain existence of saddle points in the space of parameters², nor the desirable properties of Theorem 1. Some results on the existence of saddle points in infinite action games are known, but they require properties like convexity and concavity of utility functions (Aubin, 1998), which we cannot apply as they would need to hold w.r.t. the neural network parameters. This is why the notion of *local Nash equilibrium (LNE)* has arisen in the literature (Ratliff et al., 2013; Unterthiner et al., 2018). Roughly, an LNE is a strategy profile where neither player can improve in a small neighborhood of the profile.³

¹ Note that in game theory the term 'saddle point' is used to denote a 'global' saddle point which corresponds to a Nash equilibrium: there is no profitable deviation near or far away from the current point. In contrast, in machine learning, the term 'saddle point' typically denotes a 'local' saddle point: no player can improve its payoff by making a small step from the current joint strategy.

² Note that Goodfellow et al. (2014)'s theoretical results on the existance of an equilibrium are "done in a non-parametric setting" which studies "convergence in the space of probability density functions", not parameters.

³So this corresponds to a 'local saddle point'. Cf. footnote 1.

In finite games every LNE is an NE, as, whenever there is a global deviation (i.e., a better response), one can always deviate locally in the space of mixed strategies towards a pure best response (by playing that better response with ϵ higher probability).

3. GANGs

In order to capitalize on the insight that we can escape local equilibria by switching to mixed strategy space for a finite game, we formalize adversarial networks in a (finite) games setting, that we call (finite) *Generative Adversarial Network Games (GANGs)*.

We start with making explicit how general (infinite) GANs correspond to strategic games, via the GANG framework:

Definition 5 (GANG). A *GANG* is a tuple $\mathcal{M} = \langle p_d, \langle G, p_z \rangle, C, \phi \rangle$ with

- $p_d(x)$ is the distribution over ('true' or 'real') data points $x \in \mathbb{R}^d$.
- G is a neural network class parametrized by a parameter vector $\theta_G \in \Theta_G$ and d outputs, such that $G(z; \theta_G) \in \mathbb{R}^d$ denotes the ('fake' or 'generated') output of G on a random vector z drawn from some distribution $z \sim p_z$.
- C is a neural network class parametrized by a parameter vector $\theta_C \in \Theta_C$ and a single output, such that the output $C(x;\theta_C) \in [0,1]$ indicates the 'realness' of x according to C.
- φ: [0,1] → ℝ is a measuring function (Arora et al., 2017)—e.g., log for GANs, the identity mapping for WGANs—used to specify game payoffs, explained next.

A GANG induces a zero-sum game in an intuitive way:

Definition 6. The induced zero-sum strategic-form game of a GANG is $\langle \mathcal{D} = \{G, C\}, \{\mathcal{S}_G, \mathcal{S}_C\}, \{u_G, u_C\} \rangle$ with:

- $S_G = \{G(\cdot; \theta_G) \mid \theta_G \in \Theta_G\}$ the set of strategies s_G ;
- $S_C = \{C(\cdot; \theta_C) \mid \theta_C \in \Theta_C\}$, the set of strategies s_C ;
- $u_C(s_G, s_C) = \mathbf{E}_{x \sim p_d}[\phi(s_C(x))] \mathbf{E}_{z \sim p_z}[\phi(s_C(s_G(z)))]$. I.e., the score of C is the expected 'measured realness' of the real data minus that of the fake data:
- $u_G(s_G, s_C) = -u_C(s_G, s_C)$.

As such, when using $\phi = \log$, GANGs employ a payoff function for G that use Goodfellow et al. (2014)'s trick to enforce strong gradients early in the training process, but it applies this transformation to u_C too, in order to retain the zero-sum property. The correctness of these transformations are proven in Appendix A.

In practice, GANs are represented using floating point num-

bers, of which, for a given setup, there is only a finite (albeit large) number. In GANGs, we formalize this:

Definition 7. Any GANG where G, C are finite classes—i.e., classes of networks constructed from a finite set of node types (e.g., {Sigmoid, ReLu, Linear})—and with architectures of bounded size, is called a *finite network class GANG*. A finite network class GANG in which the sets Θ_G, Θ_C are finite too, it is called a *finite GANG*.

From now on, we will focus on finite GANGs. We emphasize this finiteness, because this is exactly what enables us to obtain the desirable properties mentioned in Section 2: existence of (one or infinitely many) mixed NEs with the same value, as well as the guarantee that any LNE is an NE. Moreover, these properties hold for the GANG in its original formulation—not for a theoretical abstraction in terms of (infinite capacity) densities—which means that we can truly expect solution methods (that operate in the parametric domain) to exploit these properties. However, since we do not impose any additional constraints or discretization⁴, the number of strategies (all possible unique instantiations of the network class with floating point numbers) is huge. Therefore, we think that finding (near-) equilibria with small supports is one of the most important challenges for making principled advances in the field of adversarial networks. As a first step towards addressing this challenge, we propose to make use of the Parallel Nash Memory (PNM) (Oliehoek et al., 2006), which can be seen as a generalization (to nonexact best responses) of the double oracle method (McMahan et al., 2003).

4. Resource-Bounded GANGs

While finite GANGs do not suffer from LNEs, solving them is non-trivial: even though we know that there always is a direction (i.e., a best response) that we can play more frequently to move towards an NE, computing that direction itself is a computationally intractable task. There is huge number of candidate strategies and the best-response payoff is a non-linear (or convex) function of the chosen strategy. This means that finding an NE, or even an ϵ -NE will be typically beyond our capabilities. Therefore we consider players with bounded computational resources.

Resource-Bounded Best-Responses (RBBR). A Nash equilibrium is defined by the absence of better responses for any of the players. As such, best response computation is a critical tool to verify whether a strategy profile is an NE,

⁴ Therefore, our finite GANGs have the same representational capacity as normal GANs that are implemented using floating point arithmetic. When strategies would be highly non-continuous functions of θ_G and θ_C , then a discretization (e.g., a floating point system) might be inadequate, but then GANs are not appropriate either: neural networks are continuous functions.

and is also a common subroutine in algorithms that compute an NE.⁵ However, since computing an $(\epsilon$ -)best response will generally be intractable for GANGs, we examine the type of solutions that we actually can expect to compute with bounded computational power by the notion of *resource-bounded best response* and show how it naturally leads to the *resource-bounded NE (RB-NE)* solution concept.

We say that $S_i^{RB} \subseteq S_i$ is the subset of strategies of player i, that i can compute as a best response, given its bounded computational resources. This computable set is an abstract formulation that can capture gradient descent being trapped in local optima, as well as other phenomena that prevent us from computing a best response (e.g., not even reaching a local optimum in the available time).

Definition 8. A strategy $s_i \in \mathcal{S}_i^{RB}$ of player i is a resource-bounded best-response (RBBR) against a (possibly mixed) strategy μ_j , if $\forall s_i' \in \mathcal{S}_i^{RB}, \ u_i(s_i, \mu_j) \geq u_i(s_i', \mu_j)$.

That is, s_i only needs to be amongst the best strategies that player i can compute in response to μ_j . We denote the set of such RBBRs to μ_j by $\mathcal{S}_i^{RBBR(\mu_j)} \subseteq \mathcal{S}_i^{RB}$.

Definition 9. A resource-bounded best-response function $f_i^{RBBR}: \Delta(\mathcal{S}_j) \to \mathcal{S}_i^{RB}$ is a function that maps from the set of possible strategies of player j to an RBBR for i, s.t. $\forall_{\mu_j} \ f_i^{RBBR}(\mu_j) \in \mathcal{S}_i^{RBBR(\mu_j)}$.

Using RBBRs, we define an intuitive specialization of NE:

Definition 10. $\mu = \langle \mu_i, \mu_j \rangle$ is a resource-bounded NE (RB-NE) iff $\forall i \quad u_i(\mu_i, \mu_j) \geq u_i(f_i^{RBBR}(\mu_j), \mu_j)$.

That is, an RB-NE can be thought of as follows: we present μ to each player i and it gets the chance to switch to another strategy, for which it can apply its bounded resources (i.e., use f_i^{RBBR}) exactly once. After this application, the player's resources are exhausted and if the found $f_i^{RBBR}(\mu_j)$ does not lead to a higher payoff it will not have an incentive to deviate.⁶

Clearly, an RB-NE can be linked to the familiar notion of ϵ -NE by making assumptions on the power of the best response computation.

Theorem 2. If both players are powerful enough to compute ϵ -best responses, then an RB-NE is an ϵ -NE.

Proof. Starting from the RB-NE (μ_i, μ_j) , assume an arbitrary i. By definition of RB-NE $u_i(\mu_i, \mu_j) \geq u_i(f_i^{RBBR}(\mu_j), \mu_j) \geq \max_{\mu_i'} u_i(\mu_i', \mu_j) - \epsilon$.

Non-deterministic Best Responses. The above definitions assumed deterministic RBBR functions f_i^{RBBR} . However, in many cases the RBBR function can be non-deterministic (e.g., due to random restarts), which means that the sets \mathcal{S}_i^{RB} are non-deterministic. This is not a fundamental problem, however, and the same approach can be adapted to allow for such non-determinism.

In particular, now let f_i^{RBBR} be a non-deterministic function, and $define\ \mathcal{S}_i^{RB}$ as the range of this function. That is, we define \mathcal{S}_i^{RB} as that set of strategies that our non-deterministic RBBR function might deliver. Given this modification the definition of the RB-NE remains unchanged: a strategy profile $\mu = \langle \mu_i, \mu_j \rangle$ is a non-deterministic RB-NE if each player i uses all its computational resources by calling $f_i^{RBBR}(\mu_j)$ once, and no player finds a better strategy to switch to.

5. Solving GANGs

Treating GANGs as finite games in mixed strategies permits building on existing tools and algorithms for these classes of games (Fudenberg and Levine, 1998; Rakhlin and Sridharan, 2013a; Foster et al., 2016). In this section, we describe how to use the Parallel Nash Memory (Oliehoek et al., 2006), which explicitly aims to prevent forgetting, is particularly tailored to finding approximate NEs with small support, and monotonically⁷ converges to such an equilibrium.

In the following, we give a concise description of a slightly simplified form of Parallel Nash Memory (PNM) and how we apply it to GANGs. For ease of explanation, we focus on the setting with deterministic best responses.⁸

The algorithm is shown in Algorithm 1. Intuitively, PNM

⁵ We motivate the need for an alternative solution concept. We acknowledge the fact that there are solution methods that do not require the explicit computation for best responses, but are not aware of any such methods that would be scalable to the huge strategy spaces of finite GANGs.

⁶ Of course, during training the RBBR functions will be used many times, and therefore the overall computations that *we, the designers* ('GANG trainers'), use is a multitude of the computational capabilities that that the RB-NE assumes. However, this is of no concern: the goal of the RB-NE is to provide a characterization of the end point of training. In particular, it allows us to give an abstract formalization of the idea that more computational resources imply a better solution.

⁷ For an explanation of the precise meaning of monotonic here, we refer to Oliehoek et al. (2006). Roughly, we will be 'secure' against more strategies of the other agent with each iteration. This does not imply that the worst case payoff for an agent also improves monotonicaly. The latter property, while desirable, is not possible with an approach that incrementally constructs sub-games of the full game, as considered here: there might always be a part of the game we have not seen yet, but which we might discover in the future that will lead to a very poor worst case payoff for one of the agents.

 $^{^8}$ In our experiments, we use random initializations for the best responses. To deal with this non-determinism we simply discard any tests that are not able to find a positive payoff over the current mixed strategy NE $\langle \mu_G, \mu_C \rangle$, but we do not terminate. Instead, we run for a pre-specified number of iterations.

Algorithm 1 Parallel Nash Memory for GANGS WITH DETERMINISTIC RBBRS

```
1: \langle s_G, s_C \rangle \leftarrow \text{INITIALSTRATEGIES}()
 2: \langle \mu_G, \mu_C \rangle \leftarrow \langle \{s_G\}, \{s_C\} \rangle

⊳ set initial mixtures

 3:
     while True do
 4:
           s_G \leftarrow \text{RBBR}(\mu_C)
                                                 ⊳ get new bounded best resp.
 5:
           s_C \leftarrow \text{RBBR}(\mu_G)
 6:
           // Expected payoffs of these 'tests' against mixture:
 7:
           u_{BRs} \leftarrow u_G(s_G, \mu_C) + u_C(\mu_G, s_C)
 8:
           if u_{BRs} \leq 0 then
 9:
                break
10:
           end if
11:
           SG \leftarrow AUGMENTGAME(SG, s_G, s_C)
           \langle \mu_G, \mu_C \rangle \leftarrow \text{SOLVEGAME}(SG)
12:
13:
     end while
14: return \langle \mu_G, \mu_C \rangle
                                                              ⊳ found an BR-NE
```

incrementally grows a strategic game SG, over a number of iterations, using the AUGMENTGAME function. It uses SOLVEGAME to compute (via linear programming, see, e.g., Shoham and Leyton-Brown (2008)) a mixed strategy NE $\langle \mu_G, \mu_C \rangle$ of this smaller game at the end of each iteration. In order to generate new candidate strategies to include in SG, at the beginning of each iteration the algorithm uses a 'search' heuristic to deliver new promising strategies. In our GANG setting, we use the resource-bounded best-response (RBBR) functions of the players for this purpose. After having found new strategies, we test if they 'beat' the current $\langle \mu_G, \mu_C \rangle$, if they do, $u_{BRs} > 0$, and the game is augmented with these and solved again to find a new NE of the sub-game SG. If they do not, $u_{BRs} \leq 0$, and the algorithm stops.⁹

In order to augment the game, PNM evaluates (by simulation) each newly found strategy for each player against all of the existing strategies of the other player, thus constructing a new row and column for the maintained payoff matrix.

In order to implement the best response functions, any existing neural network architectures can be used. However, we need to compute RBBRs against *mixtures* of networks of the other player. For C this is trivial: we can simply generate a batch of fake data from the mixture μ_G . Implementing an RBBR for G against μ_C is slightly more involved, as we need to back-propagate the gradient from all the different $s_C \in \mu_C$ to G. Intuitively, one can think of a combined network consisting of the G network with its outputs connected to every $s_C \in \mu_C$ (see Figure 1). The predictions \hat{y}_{s_C} of these components $s_C \in \mu_C$ are combined in a single linear

output node $\hat{y} = \sum_{s_C \in \mu_C} \mu_C(s_C) \cdot \hat{y}_{s_C}$. This allows us to evaluate and backpropagate through the entire network. A practical implementation that avoids memory concerns instead loops through each component $s_C \in \mu_C$ and does the evaluation of the weighted prediction $\mu_C(s_C) \cdot \hat{y}_{s_C}$ and subsequent backpropagation per component.

Intuitively, it is clear that PNM converges to an RB-NE, which we now prove formally.

Theorem 3. *If PNM terminates, it has found an RB-NE.*

Proof. We show that $u_{BRs} \leq 0$ implies we have an RB-NE:

$$u_{BRs} = u_G(f_G^{RBBR}(\mu_C), \mu_C) + u_C(\mu_G, f_C^{RBBR}(\mu_G))$$

$$\leq 0 = u_G(\mu_G, \mu_C) + u_C(\mu_G, \mu_C)$$
(1)

Note that, per Def. 8, $u_G(f_G^{RBBR}(\mu_C), \mu_C) \geq u_G(s_G', \mu_C)$ for all computable $s_G' \in \mathcal{S}_G^{RB}$ (and similar for C). Therefore, the only way that $u_G(f_G^{RBBR}(\mu_C), \mu_C) \geq u_G(\mu_G, \mu_C)$ could fail to hold, is if μ_G would include some strategies that are not computable (not in \mathcal{S}_G^{RB}) that provide higher payoff. However, as the support of μ_G is composed of strategies computed in previous iterations, this cannot be the case. We conclude $u_G(f_G^{RBBR}(\mu_C), \mu_C) \geq u_G(\mu_G, \mu_C)$ and similarly $u_C(\mu_G, f_G^{RBBR}(\mu_G)) \geq u_C(\mu_G, \mu_C)$. Together with (1) this directly implies $u_G(\mu_G, \mu_C) = u_G(f_G^{RBBR}(\mu_C), \mu_C)$ and $u_C(\mu_G, \mu_C) = u_G(f_G^{RBBR}(\mu_C), \mu_C)$ indicating we found an RB-NE. \square

Corollary 1. Algorithm 1 terminates and monotonically converges to an equilibrium.

Proof. This follows directly from the fact that there are only finitely many RBBRs and the fact that we never forget RBBRs that we computed before, thus the proof for PNM (Oliehoek et al., 2006) extends to Algorithm 1. □

The PNM algorithm for GANGs is parameter free, but we mention two adaptations that are helpful.

Interleaved training of best responses. In order to speed up convergence of PNM, it is possible to train best responses of G and C in parallel, giving G access to the intermediate results of f_C^{RBBR} . This reduces the number of needed PNM iterations, but does not seem to affect the quality of the found solutions, as demonstrated in Appendix D. The results shown in the main paper do not employ this trick.

Regularization of classifier best responses. In initial experiments, we found that the best-responses by C tended to overfit—see the supplement for an extensive analysis. In order to regularize best responses for C, in each iteration, in the experiments below we sample additional data points x uniformly from a bounding box enclosing the current data

⁹ Essentially, this is the same as the double oracle method, but it replaces exact best-response computation with approximate RBBRs. Therefore, we refer to this as PNM, since that inherently allows for approximate/heuristic methods to deliver new 'test' strategies (Oliehoek et al., 2006). It also enables us to develop a version for *non-deterministic* RBBRs, by literally adopting the PNM algorithm.

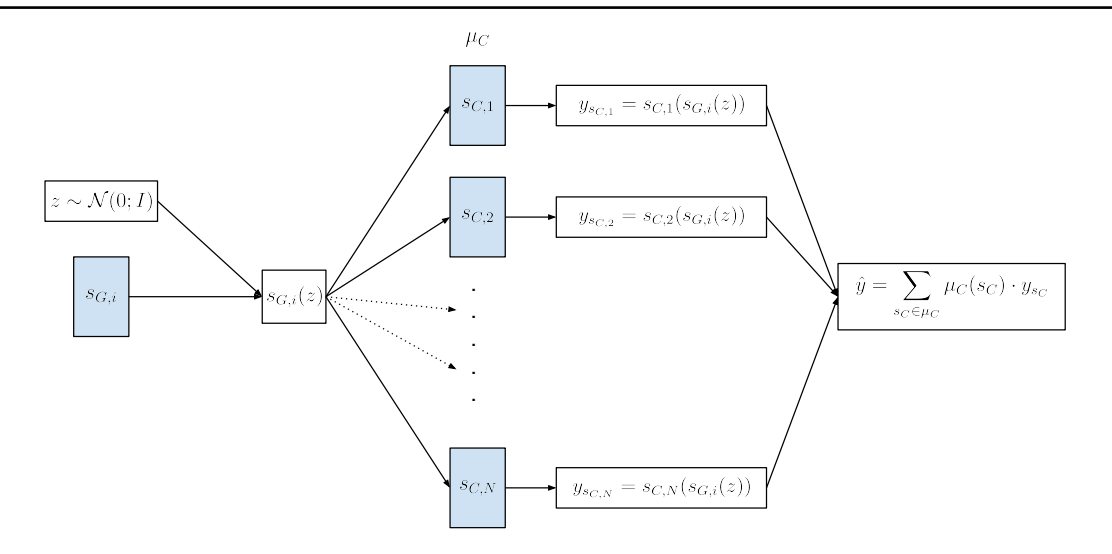


Figure 1: Network architecture that allows gradients from $s_C \in \mu_C$ to be back-propagated to G.

(both real and fake), and include these data points as additional fake data for training C. The number of 'uniform fake points' chosen coincides with the batch size used for training.

6. Experiments

Here we report on experiments that aim to test if searching in mixed strategies with PNM-GANG can help in reducing problems with training GANs, and if the found solutions (near-RB-NEs) provide better generative models and are potentially closer to true Nash equilibria than those found by GANs (near-LNEs). Since our goal is to produce better generative models, we refrain from evaluating these methods on complex data like images: image quality and log likelihood are not aligned as for instance shown by Theis et al. (2016). Moreover there is debate about whether GANs are overfitting (memorizing the data) and assessing this from samples is difficult; only crude methods have been proposed e.g., (Arora and Zhang, 2017; Salimans et al., 2016; Odena et al., 2017; Karras et al., 2018), most of which provide merely a measure of variability, not over-fitting. As such, we choose to focus on irrefutable results on mixture of Gaussian tasks, for which the distributions can readily be visualized, and which themselves have many applications.

Experimental setup. We compare our PNM approach ('PNM-GANG') to a vanilla GAN implementation and state-of-the-art MGAN (Hoang et al., 2018). Detailed training and architecture settings are summarized in the appendix.

The mixture components comprise grids and annuli with equal-variance components, as well as non-symmetric cases with randomly located modes and with a random covariance matrix for each mode. For each domain we create test cases with 9 and 16 components. In our plots, black points are real data, green points are generated data. Blue indicates areas that are classified as 'realistic' while red indicates a 'fake' classification by C.

Found solutions. The results produced by regular GANs and PNM-GANGs are shown in Figure 2 and clearly convey three main points:

- The PNM-GANG mixed classifier has a much flatter surface than the classifier found by the GAN. Around the true data, the GANG classifier outputs around 0.5 indicating indifference, which is in line with the theoretical predictions about the equilibrium (Goodfellow et al., 2014).
- 2. We see that this flatter surface is not coming at the cost of inaccurate samples. In contrast: nearly all samples shown are hitting one of the modes and thus *the PNM-GANG solutions are highly accurate*, much more so than the GANs' solutions.
- 3. Finally, the PNM-GANGs, unlike GANs, *do not suffer from mode omission*; they leave out no modes. We also note that PNM-GANG typically achieved these results with fewer total parameters than the regular GAN, e.g., 1463 vs. 7653 for the random 9 task in Figure 2.

This shows that, qualitatively, the use of multiple generators seems to lead to good results. This is corroborated by results we obtained using MGANs (illustrations and complete description can be found in Appendix C.2), which only failed to represent one mode in the 'random' task.

Impact of generator learning rate. The above results show that PNM-GANG can accurately cover multiple

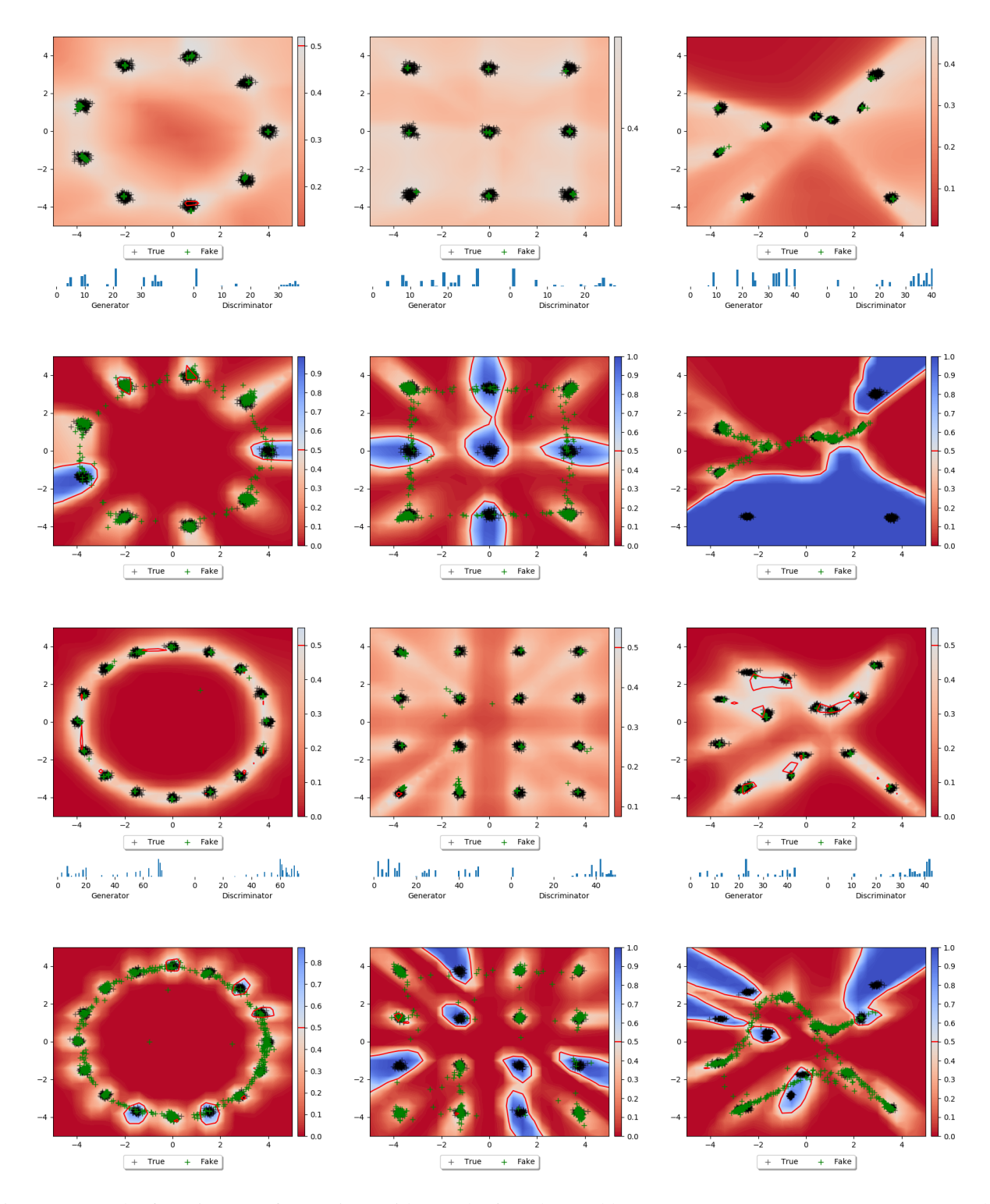


Figure 2: Results for mixtures of Gaussians with 9 and 16 modes. Odd rows: PNM-GANG, Even rows: GAN. The histograms represent the probabilities in the mixed strategy of each player. True data is shown in black, while fake data is green. The classification boundary (where the classifier outputs 0.5) is indicated with a red line. Best seen in color.

modes, however, not all modes are *fully* covered. As also pointed out by Arjovsky et al. (2017), the best response of G against μ_C is a single point with the highest 'realness', and therefore the WGAN they introduced uses fewer iterations for G than for G. Inspired by this, we investigate if we can reduce the mode collapse by reducing the learning rate of G. The results in Figure 3 show that more area of the modes are covered confirming this hypothesis. However, it also makes clear that by doing so, we are now generating some data outside of the true data, so this is a trade-off. We point out that also with total mode degeneration (where modes collapse to Dirac delta peaks), the PNM mechanism theoretically would still converge, by adding in ever more delta peaks covering parts of the modes.

Exploitability of solutions. Finally, to complement the above qualitative analysis, we also provide a quantitative analysis of the solutions found by GANs, MGANs and PNM-GANGs. We investigate to what extent they are exploitable by newly introduced adversaries with some fixed computational power (as modeled by the complexity of the networks we use to attack the found solution).

In particular, for a given solution $\tilde{\mu} = (\tilde{\mu_G}, \tilde{\mu_C})$ we use the following measure of exploitability:

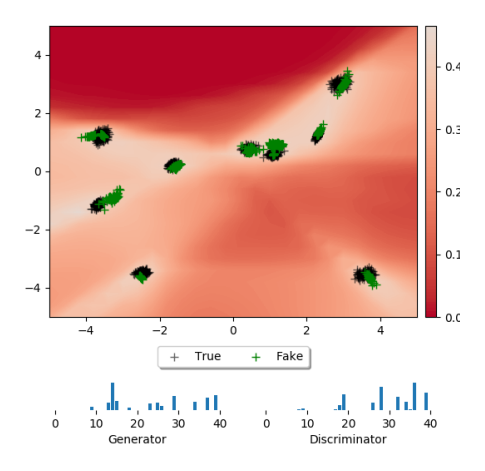
$$\begin{split} expl^{RB}(\tilde{\mu_G}, \tilde{\mu_C}) &\triangleq \mathsf{RBmax}_{\mu_G} u_G(\mu_G, \tilde{\mu_C}) \\ &+ \mathsf{RBmax}_{\mu_G} u_C(\tilde{\mu_G}, \mu_C), \end{split} \tag{2}$$

where 'RBmax' denotes an approximate maximization performed by an adversary of some fixed complexity.

That is, the 'RBmax' functions are analogous to the f_i^{RBBR} functions employed in PNM, but the computational resources of 'RBmax' could be different from those used for the f_i^{RBBR} . Intuitively, it gives a higher score if $\tilde{\mu}$ is easier to exploit. However, it is not a true measure of distance to an equilibrium: it can return values that are lower than zero which indicate that $\tilde{\mu}$ could not be exploited by the approximate best responses.

Our exploitability is closely related to the use of GAN training metrics (Im et al., 2018), but additionally includes the exploitability of the classifier. This is important: when only testing the exploitability of the generator, this does give a way to compare generators, but it does not give a way to assess how far from equilibirum we might be. Since finite GANGs are zero-sum games, distance to equilibrium is the desired performance measure. In particular, the exploitability of the classifier actually may provide information about the quality of the generator: if the generator holds up well against a perfect classifier, it should be close to the data distribution. For a further motivation of this measure of exploitability, please see Appendix B.2.

We perform two experiments on the 9 random modes task;



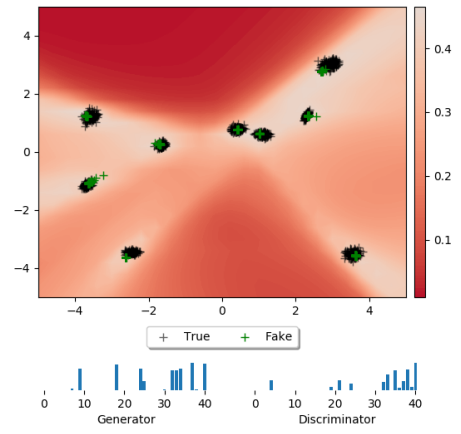
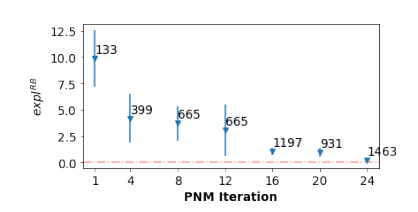


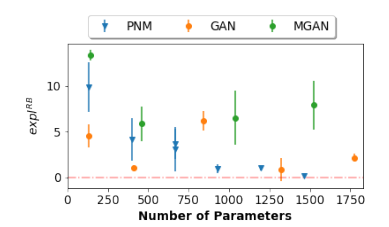
Figure 3: Results for PNM with a learning rate of 7^{-4} for the generator (top). Compare with previous result (bottom, duplicated from the first row of Figure 2).

results for other tasks are in Appendix C.2. First, we investigate the exploitability of solutions delivered by GANs, MGANs and GANGs of different complexities (in terms of *total* number of parameters used). For this, we compute 'attacks' (approximate best responses) to these solutions using attackers of fixed complexity (a total of 453 parameters for the attacking G and C together).

These results are shown in Figure 4 (left and middle). The left plot shows the exploitability of PNM-GANG after different numbers of iterations, as well as the number of parameters used in the solutions found in those iterations (a sum over all the networks in the support of the mixture). Error bars indicate standard deviation. It is apparent that PNM-GANG solutions with more parameters typically are less exploitable. Also shown is that the variance of exploitability depends heavily on the solution that we happen to attack.

The middle plot shows those same results together with exploitability results we obtained for GANs and MGANs of different complexities (all were trained to convergence).





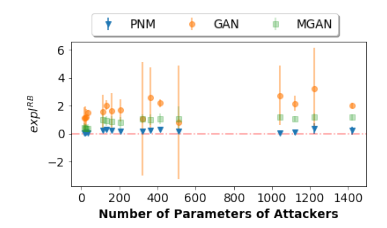


Figure 4: Exploitability results for the nine randomly located modes task. Left: exploitability of PNM-GANGs of various complexities (indicated numbers) found in different iterations. Middle: comparison of exploitability of PNM-GANGs, GANs and MGAN of various complexities. Right: exploitability of PNM-GANGs, GANs and MGAN, when varying the complexity of the attacking 'RBmax' functions. Complexities are expressed in total number of parameters (for *G* and *C* together). See text for detailed explanation of all.

Note that here the x-axis shows the complexity in terms of total parameters. The figure shows an approximately monotonic decrease in exploitability for GANGs for increasing number of parameters, while GANs and MGANs with higher complexity are still very exploitable. In contrast to GANGs, more complex architectures for GANs or MGANs are thus by no means a way to guarantee a better solution.

Secondly, we investigate what happens for the converged GAN / PNM-GANG solution of Figure 2, which have comparable complexities, when attacked with varying complexity attackers. We also employ an MGAN which has a significantly larger number of parameters (see Appendix C.2). These results are shown in Figure 4 (right). Clearly shown is that the PNM-GANG is robust with near-zero exploitability even when attacked with high complexity attackers. The MGAN solution has a non-zero level of exploitability, roughly constant for several attacker complexities. In stark contrast, we see that the converged GAN solution is exploitable already for low-complexity attackers, again suggesting that the GAN was stuck in an LNE far away from a global NE.

Overall, these results demonstrate that GANGs can provide more robust solutions than GANs/MGANs with the same number of parameters, suggesting that they are closer to a Nash equilibrium and provide better generative models.

7. Related work

Progress in zero-sum games. Bosanský et al. (2014) devise a double-oracle algorithm for computing exact equilibria in extensive-form games with imperfect information. Their algorithm uses *best-response oracles*; PNM does so too, though in this paper using resource-bounded rather than exact best responses. Lanctot et al. (2017) generalize to non-exact sub-game routines. Inspired by GANs, Hazan et al. (2017) deal with general zero-sum settings with nonconvex loss functions. They introduce a weakening of local equilibria known as *smoothed local equilibria* and provide

algorithms with guarantees on the smoothed local regret. In contrast, we introduce a generalization of local equilibrium (RB-NE) that allows for stronger notions of equilibrium, not only weaker ones, depending on the power of the RBBR functions. For the more restricted class of convex-concave zero-sum games, it was recently shown that Optimistic Mirror Descent (a variant of gradient descent) and its generalization Optimistic Follow-the-Regularized-Leader achieve faster convergence rates than gradient descent (Rakhlin and Sridharan, 2013a;b). These algorithms have been explored in the context of GANs by Daskalakis et al. (2018). However, the convergence results do not apply as GANs are not convex-concave.

GANs. The literature on GANs has been growing at an incredible rate, and a full overview of all the related works such as those by Arjovsky et al. (2017); Arjovsky and Bottou (2017); Huszár (2015); Nowozin et al. (2016); Dai et al. (2017); Zhao et al. (2017); Arora and Zhang (2017); Salimans et al. (2016); Gulrajani et al. (2017); Radford et al. (2015) is beyond the scop of this paper. Instead we refer to Unterthiner et al. (2018) for a reasonable comprehensive recent overview.

Unterthiner et al. (2018) introduce Coulomb GANs and show convergence for them but only under the strong assumption that the "generator samples can move freely" (which is not the case when training via gradient descent; samples can only move small steps). Moreover, their approach essentially performs non-parametric density estimation, which is based on the (Euclidean) distance between data points, which we believe undermines one of the most attractive features of GANs (not needing a distance metric).

Karras et al. (2018), like PNM, incrementally grow the complexity of the maintained models, but, unlike PNM, do not maintain a mixture. Many of the techniques designed to improve GAN training, e.g., (Salimans et al., 2016; Gulrajani et al., 2017; Sønderby et al., 2017; Creswell et al., 2018), concern modifications to the update for one or both players. Such techniques can directly be used in GANGs by adapting

the best response computation.

Explicit representations of mixtures of strategies. Recently, more researchers have investigated the idea of (more or less) explicitly representing a set or mixture of strategies for the players. For instance, Jiwoong Im et al. (2016) retains sets of networks that are trained by randomly pairing up with a network for the other player thus forming a GAN. This, like PNM, can be interpreted as a coevolutionary approach, but unlike PNM, it does not have any convergence guarantees.

MAD-GAN (Ghosh et al., 2017) uses k generators, but one discriminator. MGAN (Hoang et al., 2018) proposes mixtures of k generators, a classifier and a discriminator with weight sharing; and presents a theoretical analysis similar to Goodfellow et al. (2014) assuming infinite capacity densities. Unlike PNM, none of these approaches have convergence guarantees.

Generally, explicit mixtures can bring advantages in two ways: (1) Representation: intuitively, a mixture of k neural networks could better represent a complex distribution than a single neural network of the same size, and would be roughly on par with a single network that is k times as big. Arora et al. (2017) show how to create such a bigger network that is particularly suitable for dealing with multiple modes using a 'multi-way selector'. In our experiments we observed mixtures of simpler networks leading to better performance than a single larger network of the same total complexity (in terms of number of parameters). (2) Training: Arora et al. use an architecture that is tailored to representing a mixture of components and train a single such network. We, in contrast, explicitly represent the mixture; given the observation that good solutions will take the form of a mixture. This is a form of domain knowledge that facilitates learning and convergence guarantees.

The most closely related paper that we know of is the work by Grnarova et al. (2017), which also builds upon gametheoretic tools to give certain convergence guarantees. The main differences are as follows:

- 1. We provide a more general form of convergence (to an RB-NE) that is applicable to *all* architectures, that only depends on the power to compute best responses, and show that PNM-GANG converges in this sense. We also show that if agents can compute an ϵ -best response, then the procedure converges to an ϵ -NE.
- 2. Grnarova et al. (2017) show that for a quite specific GAN architecture their first algorithm converges to an ϵ -NE. On the one hand, this result is an instantiation of our more general theory: they assume they can compute exact (for G) and ϵ -approximate (for C) best responses; for such powerful players our Theorem 2 provides that

- guarantee. On the other hand, their formulation works without discretizing the spaces of strategies.
- 3. The practical implementation of their algorithm does not provide guarantees.

Bounded rationality. The proposed notion of RB-NE is one of bounded rationality (Simon, 1955). Over the years a number of different such notions have been proposed, e.g., see Russell (1997); Zilberstein (2011). Some of these also target agents in games. Perhaps the most well-known such a concept is the quantal response equilibrium (McKelvey and Palfrey, 1995). Other concepts take into account an explicit cost of computation (Rubinstein, 1986; Halpern et al., 2014), or explicitly limit the allowed strategy, for instance by limiting the size of finite-state machines that might be employed (Halpern et al., 2014). However, these notions are motivated to explain why people might show certain behaviors or how a decision maker should use its limited resources. We on the other hand, take the why and how of bounded rationality as a given, and merely model the outcome of a resource-bounded computation (as the computable set $S_i^{RB} \subseteq S_i$). In other words, we make a minimal assumption on the nature of the resource-boundedness, and aim to show that even under such general assumptions we can still reach a form of equilibrium, an RB-NE, of which the quality can be directly linked (via Theorem 2) to the computational power of the agents.

8. Conclusions

We introduce finite GANGs—Generative Adversarial Network Games—a novel framework for representing adversarial networks by formulating them as finite zero-sum games. By tackling them with techniques working in mixed strategies we can avoid getting stuck in local Nash equilibria (LNE). As finite GANGs have extremely large strategy spaces we cannot expect to exactly (or ϵ -approximately) solve them. Therefore, we introduced the resource-bounded Nash equilibrium (RB-NE). This notion is richer than LNE in that it captures not only failures of escaping local optima of gradient descent, but applies to any approximate best-response computations, including methods with random restarts.

Additionally, GANGs can draw on a rich set of methods for solving zero-sum games (Fudenberg and Levine, 1998; Rakhlin and Sridharan, 2013b; Foster et al., 2016; Oliehoek et al., 2006). In this paper, we build on PNM and prove that the resulting method monotonically converges to an RB-NE. We empirically demonstrate that the resulting method does not suffer from typical GAN problems such as mode collapse and forgetting. We also show that the GANG-PNM solutions are closer to theoretical predictions, and are less exploitable than normal GANs: by using PNM we can

train models that are more robust than GANs of the same total complexity, indicating they are closer to a global Nash equilibrium and yield better generative performance.

Future work We presented a framework that can have many instantiations and modifications. For example, one direction is to employ different learning algorithms. Another direction could focus on modifications of PNM, such as to allow discarding "stale" pure strategies, which would allow the process to run for longer without being inhibited by the size of the resulting zero-sum "subgame" that must be maintained and repeatedly solved. The addition of fake uniform data as a guiding component suggests that there might be benefit of considering "deep-interactive learning" where there is deepness in the number of players that interact in order to give each other guidance in adversarial training. This could potentially be modelled by zero-sum polymatrix games (Cai et al., 2016).

Acknowledgments

This research made use of a GPU donated by NVIDIA. F.A.O. is funded by EPSRC First Grant EP/R001227/1, and ERC Starting Grant #758824—INFLUENCE.

References

- M. Arjovsky and L. Bottou. Towards principled methods for training generative adversarial networks. In *ICLR*, 2017.
- M. Arjovsky, S. Chintala, and L. Bottou. Wasserstein generative adversarial networks. In *ICML*, 2017.
- S. Arora and Y. Zhang. Do GANs actually learn the distribution? An empirical study. *ArXiv e-prints*, June 2017.
- S. Arora, R. Ge, Y. Liang, T. Ma, and Y. Zhang. Generalization and equilibrium in generative adversarial nets (GANs). In *ICML*, 2017.
- J.-P. Aubin. Optima and equilibria: an introduction to nonlinear analysis, volume 140. Springer Science & Business Media, 1998.
- B. Bosanský, C. Kiekintveld, V. Lisý, and M. Pechoucek. An exact double-oracle algorithm for zero-sum extensiveform games with imperfect information. *Journal of AI Research*, 51, 2014.
- Y. Cai, O. Candogan, C. Daskalakis, and C. H. Papadimitriou. Zero-sum polymatrix games: A generalization of minmax. *Math. Oper. Res.*, 41(2), 2016.
- S. Chintala. How to train a GAN? tips and tricks to make GANs work. https://github.com/soumith/ganhacks, 2016. Retrieved on 2018-02-08.
- A. Creswell, T. White, V. Dumoulin, K. Arulkumaran, B. Sengupta, and A. A. Bharath. Generative adversarial

- networks: An overview. *IEEE Signal Processing Magazine*, 35(1), 2018.
- Z. Dai, A. Almahairi, P. Bachman, E. H. Hovy, and A. C. Courville. Calibrating energy-based generative adversarial networks. In *ICLR*, 2017.
- C. Daskalakis, A. Ilyas, V. Syrgkanis, and H. Zeng. Training GANs with Optimism. In *ICLR*, 2018.
- D. J. Foster, Z. Li, T. Lykouris, K. Sridharan, and E. Tardos. Learning in games: Robustness of fast convergence. In *NIPS* 29, 2016.
- D. Fudenberg and D. K. Levine. *The theory of learning in games*. MIT press, 1998.
- A. Ghosh, V. Kulharia, V. P. Namboodiri, P. H. S. Torr, and P. K. Dokania. Multi-agent diverse generative adversarial networks. *CoRR*, abs/1704.02906, 2017.
- I. Goodfellow, J. Pouget-Abadie, M. Mirza, B. Xu, D. Warde-Farley, S. Ozair, A. Courville, and Y. Bengio. Generative adversarial nets. In NIPS 27, 2014.
- P. Grnarova, K. Y. Levy, A. Lucchi, T. Hofmann, and A. Krause. An Online Learning Approach to Generative Adversarial Networks. *ArXiv e-prints*, June 2017.
- I. Gulrajani, F. Ahmed, M. Arjovsky, V. Dumoulin, and A. C. Courville. Improved training of Wasserstein GANs. *CoRR*, abs/1704.00028, 2017.
- J. Y. Halpern, R. Pass, and L. Seeman. Decision theory with resource-bounded agents. *Topics in Cognitive Science*, 6 (2), 2014. ISSN 1756-8765.
- E. Hazan, K. Singh, and C. Zhang. Efficient regret minimization in non-convex games. In *ICML*, 2017.
- M. Heusel, H. Ramsauer, T. Unterthiner, B. Nessler, and S. Hochreiter. GANs trained by a two time-scale update rule converge to a local Nash equilibrium. In *NIPS 30*, 2017.
- Q. Hoang, T. D. Nguyen, T. Le, and D. Q. Phung. Multigenerator generative adversarial nets. In *ICLR*, 2018.
- F. Huszár. How (not) to Train your Generative Model: Scheduled Sampling, Likelihood, Adversary? *ArXiv e-prints*, Nov. 2015.
- D. J. Im, A. H. Ma, G. W. Taylor, and K. Branson. Quantitatively evaluating GANs with divergences proposed for training. In *ICLR*, 2018.
- D. Jiwoong Im, H. Ma, C. Dongjoo Kim, and G. Taylor. Generative Adversarial Parallelization. *ArXiv e-prints*, Dec. 2016.
- T. Karras, T. Aila, S. Laine, and J. Lehtinen. Progressive growing of GANs for improved quality, stability, and variation. In *ICLR*, 2018.

- M. Lanctot, V. Zambaldi, A. Gruslys, A. Lazaridou, J. Perolat, D. Silver, and T. Graepel. A unified game-theoretic approach to multiagent reinforcement learning. In NIPS 30, 2017.
- W. Li, M. Gauci, and R. Groß. Turing learning: a metricfree approach to inferring behavior and its application to swarms. Swarm Intelligence, 10(3), 2016.
- L. Liu. The invariance of best reply correspondences in twoplayer games. http://www.cb.cityu.edu.hk/ ef/getFileWorkingPaper.cfm?id=193, 1996.
- R. D. McKelvey and T. R. Palfrey. Quantal response equilibria for normal form games. *Games and Economic Behavior*, 10(1), 1995. ISSN 0899-8256.
- H. B. McMahan, G. J. Gordon, and A. Blum. Planning in the presence of cost functions controlled by an adversary. In *Proceedings of the 20th International Conference on Machine Learning (ICML-03)*, pages 536–543, 2003.
- J. F. Nash. Equilibrium points in N-person games. *Proceedings of the National Academy of Sciences of the United States of America*, 36, 1950.
- S. Nowozin, B. Cseke, and R. Tomioka. f-GAN: Training generative neural samplers using variational divergence minimization. In NIPS 29, 2016.
- A. Odena, C. Olah, and J. Shlens. Conditional image synthesis with auxiliary classifier GANs. In *ICML*, 2017.
- F. A. Oliehoek, E. D. de Jong, and N. Vlassis. The parallel Nash memory for asymmetric games. In *Proc. Genetic and Evolutionary Computation (GECCO)*, 2006.
- F. A. Oliehoek, R. Savani, J. Gallego-Posada, E. van der Pol, E. D. de Jong, and R. Gross. GANGs: Generative adversarial network games. *CoRR*, abs/1712.00679, 2017. URL http://arxiv.org/abs/1712.00679.
- M. J. Osborne and A. Rubinstein. *A Course in Game Theory*, chapter Nash Equilibrium. The MIT Press, July 1994.
- A. Radford, L. Metz, and S. Chintala. Unsupervised Representation Learning with Deep Convolutional Generative Adversarial Networks. ArXiv e-prints, Nov. 2015.
- A. Rakhlin and K. Sridharan. Online learning with predictable sequences. In *Proc. of the Conference on Learning Theory*, 2013a.
- A. Rakhlin and K. Sridharan. Optimization, learning, and games with predictable sequences. In *NIPS* 26, 2013b.
- L. J. Ratliff, S. A. Burden, and S. S. Sastry. Characterization and computation of local Nash equilibria in continuous games. In *Communication, Control, and Computing*, 2013 51st Annual Allerton Conference on. IEEE, 2013.
- A. Rubinstein. Finite automata play the repeated prisoner's dilemma. *Journal of Economic Theory*, 39(1), 1986.

- S. J. Russell. Rationality and intelligence. *Artificial Intelligence*, 94(1-2), 1997.
- T. Salimans, I. J. Goodfellow, W. Zaremba, V. Cheung, A. Radford, and X. Chen. Improved techniques for training GANs. In NIPS 29, 2016.
- Y. Shoham and K. Leyton-Brown. *Multi-Agent Systems: Algorithmic, game-theoretic and logical foundations*. Cambridge University Press, 2008.
- H. A. Simon. A behavioral model of rational choice. *The Quarterly Journal of Economics*, 69(1), 1955.
- C. K. Sønderby, J. Caballero, L. Theis, W. Shi, and F. Huszár. Amortised map inference for image super-resolution. In *ICLR*, 2017.
- L. Theis, A. van den Oord, and M. Bethge. A note on the evaluation of generative models. In *ICLR*, 2016.
- T. Unterthiner, B. Nessler, G. Klambauer, M. Heusel, H. Ramsauer, and S. Hochreiter. Coulomb GANs: Provably optimal Nash equilibria via potential fields. In *ICLR*, 2018.
- J. von Neumann. Zur Theorie der Gesellschaftsspiele. *Mathematische Annalen*, 100(1), 1928.
- J. J. Zhao, M. Mathieu, and Y. LeCun. Energy-based generative adversarial network. In *ICLR*, 2017.
- S. Zilberstein. Metareasoning and bounded rationality. In M. Cox and A. Raja, editors, *Metareasoning: Thinking about Thinking*. MIT Press, 2011.

A. The zero-sum formulation of GANs and GANGs

In contrast to much of the GAN-literature, we explicitly formulate GANGs as being zero-sum games. GANs (Goodfellow et al., 2014) formulate the payoff of the generator as a function of the fake data only: $u_G = \mathbf{E}_{z \sim p_z} \left[\phi \left(1 - s_C(s_G(z)) \right) \right]$. However, it turns out that this difference typically has no implications for the sought solutions. We clarify this with the following theorem, and investigate particular instantiations below. In game theory, two games are called *strategically equivalent* if they possess exactly the same set of Nash equilibria; this (standard) definition is concerned only about the mixed strategies played in equilibrium and not the resulting payoffs. The following is a well-known game transformation (folklore, see Liu (1996)) that creates a new strategically equivalent game:

Fact 1. Consider a game $\Gamma = \langle \{1,2\}, \{S_1,S_2\}, \{u_1,u_2\} \rangle$. Fix a pure strategy $s_2 \in S_2$. Define $\bar{u_1}$ as identical to u_1 except that $\bar{u_1}(s_i,s_2) = u_1(s_i,s_2) + c$ for all $s_i \in S_1$ and some constant c. We have that Γ and $\bar{\Gamma} = \langle \{1,2\}, \{S_1,S_2\}, \{\bar{u_1},u_2\} \rangle$ are strategically equivalent.

Theorem 4. Let $Fake_C(s_G, s_C)$, and $Real_C(s_C)$ be arbitrary functions, then any finite (non-zero-sum) two-player game between G and C with payoffs of the following form:

$$u_G = Fake_G(s_G, s_C) \triangleq -Fake_C(s_G, s_C),$$

$$u_C = Real_C(s_C) + Fake_C(s_G, s_C),$$

is strategically equivalent to a zero-sum game where G has instead payoff $\bar{u_G} \triangleq -Real_C(s_C) - Fake_C(s_G, s_C)$.

Proof. By $\operatorname{adding-Real}_C(s_C)$ to G's utility function, for each pure strategy s_C of C we add a different constant to all utilities of G against s_C . Thus, by applying Fact 1 iteratively for all $s_C \in \mathcal{S}_C$ we see that we produce a strategically equivalent game.

Next, we formally specify the conversion of existing GAN models to GANGs. We consider the general measure function that covers GANs ($\phi(x) = \log(x)$) and WGANs ($\phi(x) = x - 1$). In these models, the payoffs are specified as

$$u_{G}(s_{G}, s_{C}) \triangleq -\mathbf{E}_{z \sim p_{z}} \left[\phi \left(1 - s_{C} \left(s_{G}(z) \right) \right) \right],$$

$$u_{C}(s_{G}, s_{C}) \triangleq \mathbf{E}_{x \sim p_{d}} \left[\phi \left(s_{C}(x) \right) \right] + \mathbf{E}_{z \sim p_{z}} \left[\phi \left(1 - s_{C} \left(s_{G}(z) \right) \right) \right].$$

These can be re-written using $Fake_C(s_G, s_C) = \mathbf{E}_{z \sim p_z} \left[\phi \left(1 - s_C \left(s_G(z) \right) \right) \right]$ and $Real_C(s_C) = \mathbf{E}_{x \sim p_d} \left[\phi \left(s_C(x) \right) \right]$. This means that we can employ Theorem 4 and equivalently define a GANG with zero-sum payoffs that preserves the NEs.

In practice, most work on GANs uses a different objective, introduced by Goodfellow et al. (2014). They say that [formulas altered]:

"Rather than training G to minimize $\log(1 - s_C(s_G(z)))$ we can train G to maximize $\log s_C(s_G(z))$. This objective function results in the same fixed point of the dynamics of G and G but provides much stronger gradients early in learning."

This means that they redefine $u_G(s_G, s_C) \triangleq \mathbf{E}_{z \sim p_z} \left[\phi \left(s_C \left(s_G(z) \right) \right) \right]$, which still can be written as $Fake_G(s_G, s_C) = \mathbf{E}_{z \sim p_z} \left[\phi \left(s_C \left(s_G(z) \right) \right) \right]$, which means that it is candidate for transformation to u_G . Now, as long as the classifier's payoff is also adapted we can still write the payoff functions in the form of Theorem 4. That is, the trick is compatible with a zero-sum formulation, as long as it is also applied to the classifier. This then yields:

$$u_C(s_G, s_C) = \mathbf{E}_{x \sim p_d}[\phi(s_C(x))] - \mathbf{E}_{z \sim p_z}[\phi(s_C(s_G(z)))]. \tag{3}$$

B. Experimental setup

Table 1 summarizes the settings for GAN and PNM training. As suggested by (Chintala, 2016), we use leaky ReLU as inner activation for our GAN implementation to avoid sparse gradients. Generators have linear output layers. Classifiers use sigmoids for the final layer. Both classifiers and generators are multi-layer perceptrons with 3 hidden layers. We do not use techniques such as Dropout or Batch Normalization, as they did not yield significant improvements in the quality of our experimental results. The MGAN configuration is identical to that of Table 3 in Appendix C1 of Hoang et al. (2018).

	GAN	RBBR		
Learning Rate	$3 \cdot 10^{-4}$	$5 \cdot 10^{-3}$		
Batch Size	128	128		
Z Dimension	40	5		
H Dimension	50	5		
Iterations	20000	750		
Generator Parameters	4902	92		
Classifier Parameters	2751	61		
Inner Activation	Leaky ReLU	Leaky ReLU		
Measuring Function	log	10^{-5} -bounded \log		

Table 1: Settings used to train GANs and RBBRs.

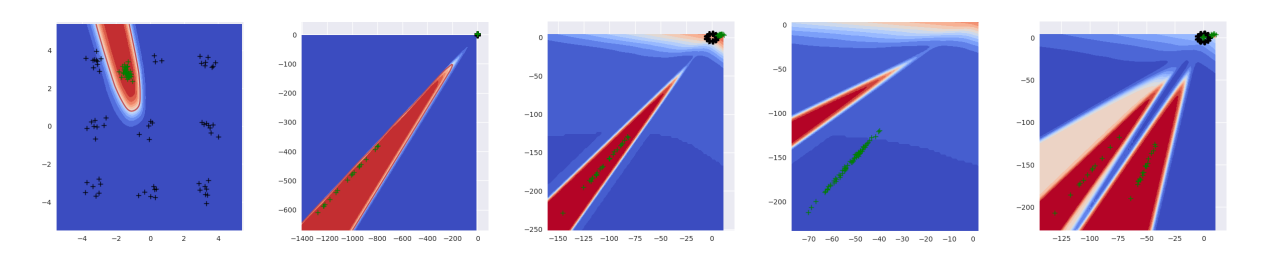


Figure 5: Illustration of exploitation of 'overfitted' classifier best-response.

B.1. Using uniform fake data to regularize classifier best responses

Plain application of PNM. In GANGs, G informs C about what good strategies are and vice versa. However, as we will make clear here, this G has limited incentive to provide the best possible training signal to C.

This is illustrated in Figure 5. The left two figures show the *same* best response by C: zoomed in on the data and zoomed out to cover some fake outliers. Clearly, C needs to find creative solutions to try and both remove the faraway points and also do good near the real data. As a result, it ends up with the shown narrow beams in an effort to give high score to the true data points (a very broad beam would lower their scores), but this exposes C to being exploited in later iterations: G needs to merely shift the samples to some other part of the vast empty space around the data.

This phenomenon is nicely illustrated by the remaining three plots (that are from a different training run, but illustrate it well): the middle plot shows an NE that targets one beam, this is exploited by G in its next best response (fourth image, note the different scales on the axes, the 'beam' is the same). The process continues, and C will need to find mixtures of all these type of complex counter measures (rightmost plot). This process can take a long time.

PNM with added uniform fake data. The GANG formalism allows us to incorporate a simple way to resolve this issue and make training more effective. In each iteration, we look at the total span (i.e., bounding box) of the real and fake data combined, and we add some uniformly sampled fake data in this bounded box (we used the same amount as fake data produced by G). In that way, we further guide C in order to better guide the generator (by directly making clear that all the area beyond the true data is fake). The impact of this procedure is illustrated by Figure 6, which shows the payoffs that the maintained mixtures μ_G , μ_C achieve against the RBBRs computed against them (so this is a measure of security), as well as the 'payoff for tests' (u_{BR}). Clearly, adding uniform fake data leads to much faster convergence. As such, we perform our main comparison to GANs with this uniform fake data component added in.

B.2. A measure of exploitability

GANGs are guaranteed to converge to an RB-NE, while GANs (in the best case) only converge to a local NE (LNE). Therefore we hypothesize that GANGs, given sufficient computational power, yield better solutions that are 'closer to a Nash equilibrium'. This is important, even in settings where we only care about the performance of the generator: by formulating the problem as a game (GAN or GANG), we have committed to approach the problem by trying to find an NE (even if that is computationally intractable).

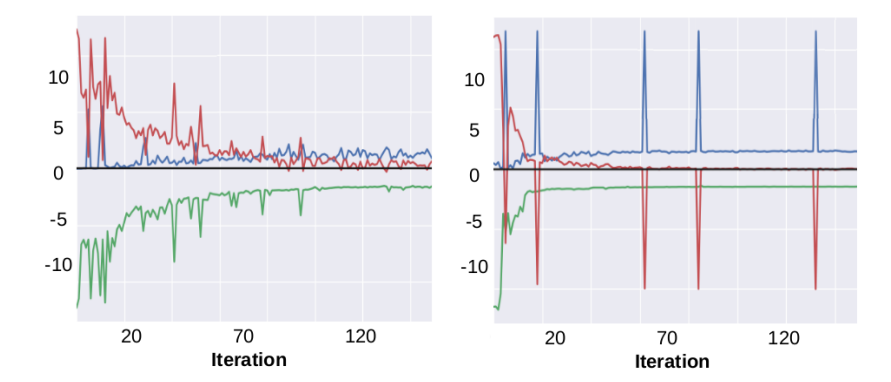


Figure 6: Convergence without (left) and with (right) adding uniform fake data. Shown is payoff as a function of the number of iterations of PNM: generator (blue), classifier (green), tests (red). The tests that do not generate positive payoff (red line < 0) are not added to the mixture.

Here we propose a measure to test how far from a Nash equilibrium we might be by measuring to what extent the found solution is exploitable by adversaries of some complexity. While this is far from a perfect measure, ourselves only being equipped with bounded computational resources, this might be the best we can do.

In particular, recall that at an NE, we realize the value of the game:

$$\min_{\mu_C} \max_{\mu_G} u_G(\mu_G, \mu_C) = \max_{\mu_G} \min_{\mu_C} u_G(\mu_G, \mu_C) = v^*$$
(4)

In other words, for an equilibrium $\langle \mu_G^*, \mu_C^* \rangle$ we have that:

$$\max_{\mu_G} u_G(\mu_G, \mu_C^*) = v^* \tag{5}$$

$$\min_{\mu_C} u_G(\mu_G^*, \mu_C) = v^* = \min_{\mu_C} -u_C(\mu_G^*, \mu_C) = -\max_{\mu_C} u_C(\mu_G^*, \mu_C)$$
(6)

which means that $\max_{\mu_C} u_C(\mu_G^*, \mu_C) = -v^*$. It also means that if we would know v^* , we would be able to say 'how far away' some found $\tilde{\mu_C}$ is from an equilibrium strategy μ_C^* (in terms of value) by looking at the *best-response exploitability*:

$$expl^{BR}(\tilde{\mu_C}) = \max_{\mu_G} u_G(\mu_G, \tilde{\mu_C}) - v^* \ge 0$$
 (7)

where the inequality holds assuming we can find the actual best response. Similarly for a μ_G we can have a look at

$$\min_{\mu_G} u_G(\tilde{\mu_G}, \mu_C) - v^* \le 0$$

I.e., if $\tilde{\mu_G}$ is an equilibrium strategy $\min_{\mu_C} u_G(\tilde{\mu_G}, \mu_C) = v^*$ but if $\tilde{\mu_G}$ is less robust, the minimum is going to be lower leading to a negative value of the expression (again assuming perfect best response μ_C). Since negative numbers are unnatural to interpret as a distance, we define (again, assuming perfect best response computation):

$$expl^{BR}(\tilde{\mu_G}) = v^* - \min_{\mu_C} u_G(\tilde{\mu_G}, \mu_C) = v^* + \max_{\mu_C} -u_G(\tilde{\mu_G}, \mu_C) = v^* + \underbrace{\max_{\mu_C} u_C(\tilde{\mu_G}, \mu_C)}_{\text{at least} = v^*} \ge 0$$
 (8)

Note that, expanding the payoff function, and realizing that the maximum will be attained at a deterministic strategy s_C :

$$expl^{BR}(\tilde{\mu_G}) = v^* + \underbrace{\max_{s_C} \left(\mathbf{E}_{x \sim p_d} \left[\phi(s_C(x)) \right] + \mathbf{E}_{z \sim p_z, z \sim \tilde{\mu_G}(z)} \left[\phi(1 - s_C(x)) \right] \right)}_{s_C},$$

which means this exploitability corresponds "to optimizing the divergence and distance metrics that were used to train the GANs" (Im et al., 2018), offset by v^* .

In the theoretical non-parametric setting (with infinite capacity densities as the strategies) this is directly useful, because then we know that the generator is able to exactly match the density, and that $v^* = \log 4$ (for the \log measuring function, which leads to a correspondence to the Jensen-Shannon divergence (Goodfellow et al., 2014)), since C will not be able to discriminate (give higher 'realness score' to) real data from on fake data.

However, this may not be a score that is attainable in finite GANG or GANs: First, there might not be a (mixture of) neural networks in the considered class that will match the data density, second there might not be classifier strategies that perfectly classify this discrepancy between the true and generated fake data. Which means that we can not deduce v^* . Therefore, even when we assume we can compute perfect best responses, in the finite setting computing these distances might not be sufficient to determine how far from a Nash equilibrium we are. Like Im et al. (2018) and others before them, one might hope that using a neural network classifier to compute a finite approximation to the aforementioned divergences and metrics., i.e., approximating $expl^{BR}(\tilde{\mu_G})$, will still give a way to compare generators (and it does), but it does not tell how far from equilibrium one is.

However, even though we do not know v^* , in the case where we can compute perfect best responses, we can compute a notion of distance of a tuple $\langle \tilde{\mu_G}, \tilde{\mu_C} \rangle$ to equilibrium by looking at the sum:

$$expl^{BR}(\tilde{\mu_G}, \tilde{\mu_C}) \triangleq expl^{BR}(\tilde{\mu_C}) + expl^{BR}(\tilde{\mu_G}) = \left(\max_{\mu_G} u_G(\mu_G, \tilde{\mu_C}) - v^*\right) + \left(v^* + \max_{\mu_C} u_C(\tilde{\mu_G}, \mu_C)\right) = \max_{\mu_G} u_G(\mu_G, \tilde{\mu_C}) + \max_{\mu_C} u_C(\tilde{\mu_G}, \mu_C) \quad (9)$$

So by reasoning about the tuple $(\tilde{\mu_G}, \tilde{\mu_C})$ rather than only $\tilde{\mu_G}$, we are able to eliminate the factor of uncertainty: v^* .

We therefore propose to take this approach, also in the case where we cannot guarantee computing best responses (the second factor of uncertainty). However, note that in (9), since both terms are guaranteed to be larger than 0, we do not need to worry about cancellations of terms and the measure will never underestimate. This is no longer the case when using approximate maximization. Still we can define a *resource-bounded* variant:

$$expl^{RB}(\tilde{\mu_G}, \tilde{\mu_C}) \triangleq (RBmax_{\mu_G}u_G(\mu_G, \tilde{\mu_C}) - v^*) + (v^* + RBmax_{\mu_C}u_C(\tilde{\mu_G}, \mu_C))$$

$$= RBmax_{\mu_G}u_G(\mu_G, \tilde{\mu_C}) + RBmax_{\mu_C}u_C(\tilde{\mu_G}, \mu_C).$$

$$(10)$$

It does not eliminate the second source of uncertainty, but neither does approximating $expl^{BR}(\tilde{\mu_G})$. This is a perfectly useful tool (a lower bound to be precise) to get some information about the distance to an equilibrium, as long as we are careful with its interpretation. In particular, since either or both of the terms of (10) could end up being lower than 0 (due to failure of computing an exact best response), we might end up underestimating the distance, and we can even get negative values. However, $expl^{RB}$ is still useful for *comparing* different found solution pairs $\langle \tilde{\mu_G}, \tilde{\mu_C} \rangle$ and $\langle \tilde{\mu_G}', \tilde{\mu_C}' \rangle$ as long as we use the same computational resources to compute approximate best responses against them. Negative values of $expl^{RB}(\tilde{\mu_G}, \tilde{\mu_C})$ should be interpreted as "robust up to our computational resources to attack it".

C. Additional empirical results

C.1. Low generator learning rate

Figure 7 shows the results of a lower learning rate for the generator for all 9 mode tasks. The general picture is the same as for the random 9 modes task treated in the main paper: the modes are better covered by fake data, but in places we see that this is at the expense of accuracy.

C.2. Exploitability results

MGAN Hoang et al. (2018) proposes a setup with a mixture of k generators, a classifier, and a discriminator. In their setting, the generator mixture aims to create samples which match the training data distribution, while the discriminator

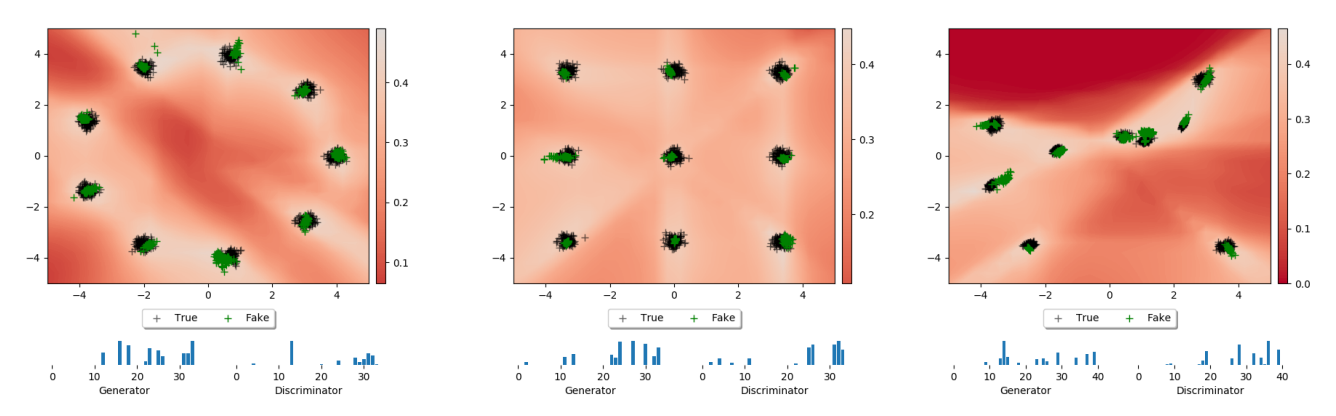


Figure 7: Results for PNM with a learning rate of 7^{-4} for the generator. Compare with the first row of Figure 2.

distinguishes real and generated samples, and the classifier tries to determine which generator a sample comes from. Similar to Goodfellow et al. (2014), MGAN presents a theoretical analysis assuming infinite capacity densities. We use MGAN as a state-of-the art baseline that was explicitly designed to overcome the problem of mode collapse.

Figure 8 shows the results of MGAN on the mixture of Gaussian tasks. MGAN results were obtained with an architecture and hyperparameters which exactly match those proposed by Hoang et al. (2018) for a similar task. This means that the MGAN models shown use many more parameters (approx. 310,000) than the GAN and GANG models (approx. 2,000). MGAN requires the number of generators to be chosen upfront as a hyperparameter of the method. We chose this to be equal to the number of mixture components, so that MGAN could cover all modes with one generator per mode. We note that PNM does not require such a hyperparameter to be set, nor does PNM require the related "diversity" hyperparameter of the MGAN method (called β in the MGAN paper).

Looking at Figure 8, we see that MGAN results do seem qualitatively quite good, even though there is one missed mode (and thus also one mode covered by 2 generators) on the randomly located components task (right column).

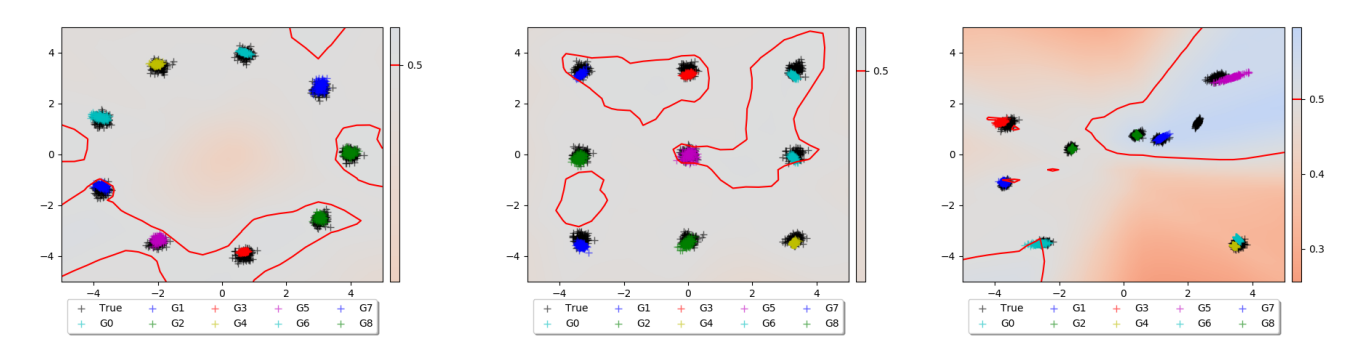


Figure 8: Results for MGAN on several mixture of Gaussian tasks with 9 modes. Markers correspond to samples created by each generator.

Figure 9 shows our exploitability results for all three tasks with nine modes. We observe roughly the same trend across the three tasks. The left column plots show the exploitability of GANG after different numbers of iterations (with respect to an attacker of fixed complexity: 453 parameters for the attacking G and C together), as well as the number of parameters used in the solutions found in those iterations (a sum over all the networks in the support of the mixture for both players). Error bars indicate standard deviations over 15 trials. Note how the exploitability of the found solution monotonically decreases as the PNM iterations increase.

The middle column shows how exploitable GAN, MGAN and PNM-GANG models of different complexities are: the x-axis indicates the total number of parameters, while the y-axis shows the exploitability. The PNM results are the same points also

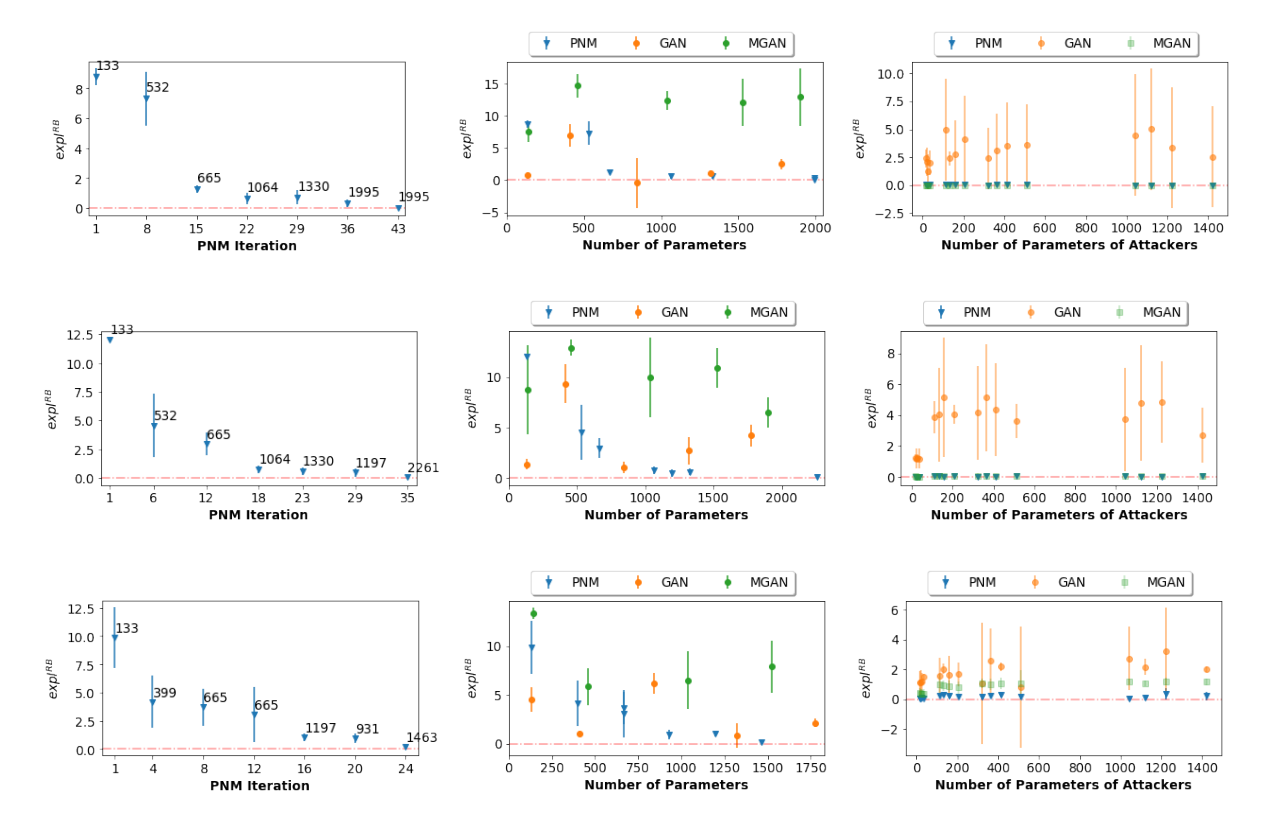


Figure 9: Exploitability results all 9 mode tasks. Top to bottom: round, grid, random.

shown in the left column, but repositioned at the appropriate place on the x-axis. All data points are exploitability of models that were trained until convergence. Note that here the x-axis shows the complexity in terms of total parameters. The figure shows an approximately monotonic decrease in exploitability for GANGs, while GANs and MGANs with higher complexity are still very exploitable in many cases. In contrast to GANGs, more complex architectures for GANs or MGANs are thus not necessarily a way to guarantee a better solution.

Additionally, we investigate the exploitability of the trained models presented in Figure 1 when attacked by neural networks of varying complexity. These results are shown in the right column of Figure 9. Clearly shown is that the PNM-GANG is robust with near-zero exploitability even when attacked with high-complexity attackers. The MGAN models also have low exploitability, but recall that these models are *much* more complex (GANG and GAN models have approximately 2,000 parameters, while the MGAN model involves approximately 310,000 parameters). Even with such a complex model, in the 'random' task, the MGAN solution has a non-zero level of exploitability, roughly constant for several attacker complexities. This is related to the missed mode and the fact that two of the MGAN generators collapsed to the same lower-right mode in Figure 1. In stark contrast to both PNM-GANGs and MGAN, we see that the converged GAN solution is exploitable already for low-complexity attackers, again suggesting that the GAN was stuck in an Local Nash Equilibrium far away from a (global) Nash Equilibrium.

As stated in the main paper, the variance of the exploitability depends critically on the solution that is attacked. The top row of Figure 10 shows the results of three different attacks of the G against the G against the G found by the GAN (top), and PNM-GANG (bottom). We see that in the top row, due to the shape of G the attacking generators reliably find the blue region with large classifier scores. On the other hand, in the bottom row, we see that the attacking generators sometimes succeed in finding a blue area, but sometimes get stuck in a local optimum (bottom left plot).

These results demonstrate that PNM-GANGs can provide more robust solutions than GANs/MGANs with the same number of parameters, suggesting that they are closer to a Nash equilibrium and provide better generative models.

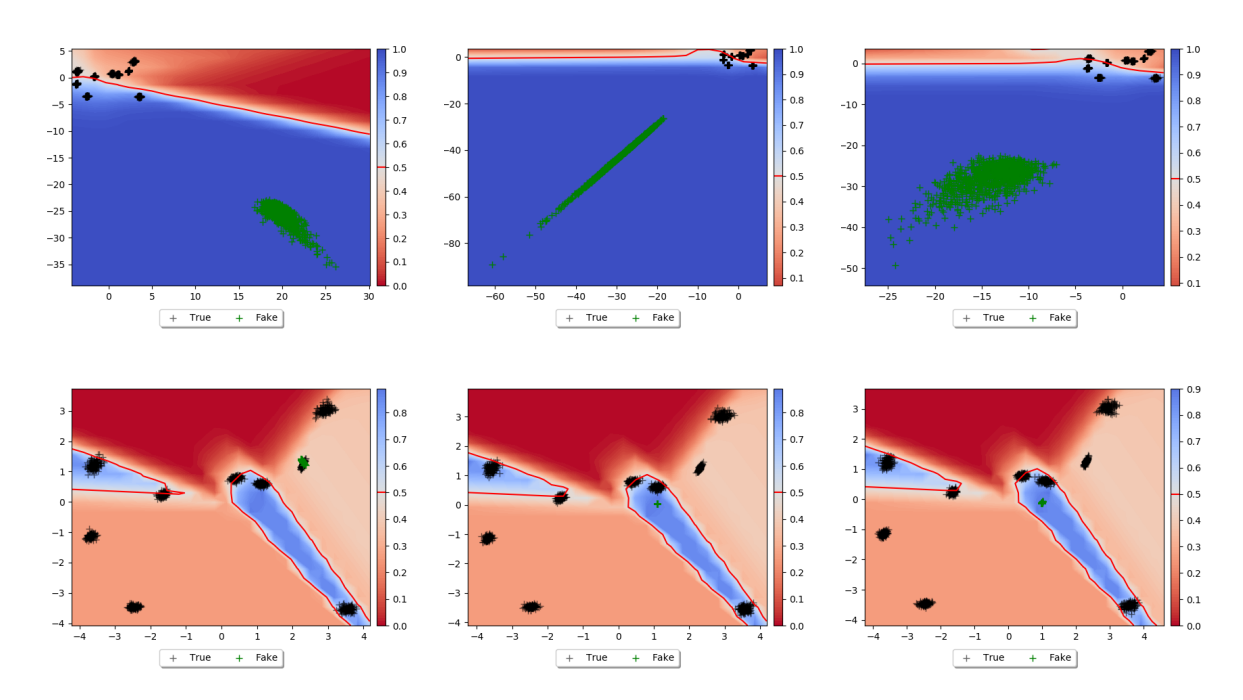


Figure 10: Found best response generators against a fixed GAN (top) and PNM-GANG (bottom) classifier.

D. Interleaved training for faster convergence

In order to speed up convergence of PNM-GANG, it is possible to train best responses of G and C in parallel, giving G access to the intermediate results of f_C^{RBBR} . The resulting algorithm is shown in Algorithm 2.

In this case, the loss with which G is trained depends not only on the scores given by the current mixture of classifiers, μ_C , but also on the classification scores given by C. Formally, the new proposed loss for G is a weighted sum of the losses if it were to be evaluated against μ_C and C, respectively. Clearly, the best response computation presented in the paper corresponds to the case in which the weight of the loss coming from C is zero. Intuitively, this gives the generator player the chance to be one-step ahead of the discriminator in discovering modes that are not being currently covered by μ_G .

This technique may interfere with the convergence guarantees provided above. It might not be the case that we are in fact computing a resource-bounded best-response for G anymore. However, in practice it performs very well: it reduces the

Algorithm 2 Interleaved Training PNM for GANGS

```
1: \langle s_G, s_C \rangle \leftarrow \text{INITIALSTRATEGIES}()
 2:
      \langle \mu_G, \mu_C \rangle \leftarrow \langle \{s_G\}, \{s_C\} \rangle

⊳ set initial mixtures

 3:
      while True do
 4:
           while Training do
 5:
                s_C \leftarrow \mathsf{GRADIENTSTEPC}(\mu_G)
                s_G \leftarrow \text{GRADIENTSTEPG}(\mu_C, s_C)
 6:
 7:
           end while
 8:
           // Expected payoffs of these 'tests' against mixture:
 9:
           u_{BRs} \leftarrow u_G(s_G, \mu_C) + u_C(\mu_G, s_C)
10:
           if u_{BRs} \leq 0 then
11:
                break
12:
           SG \leftarrow AUGMENTGAME(SG, s_G, s_C)
13:
14:
           \langle \mu_G, \mu_C \rangle \leftarrow \text{SOLVEGAME}(SG)
15: end while
16: return \langle \mu_G, \mu_C \rangle
```

number of needed PNM iteratio	ons, but does not affect th	ne quality of the found	solutions, as demonstra	ated in Figure 11.

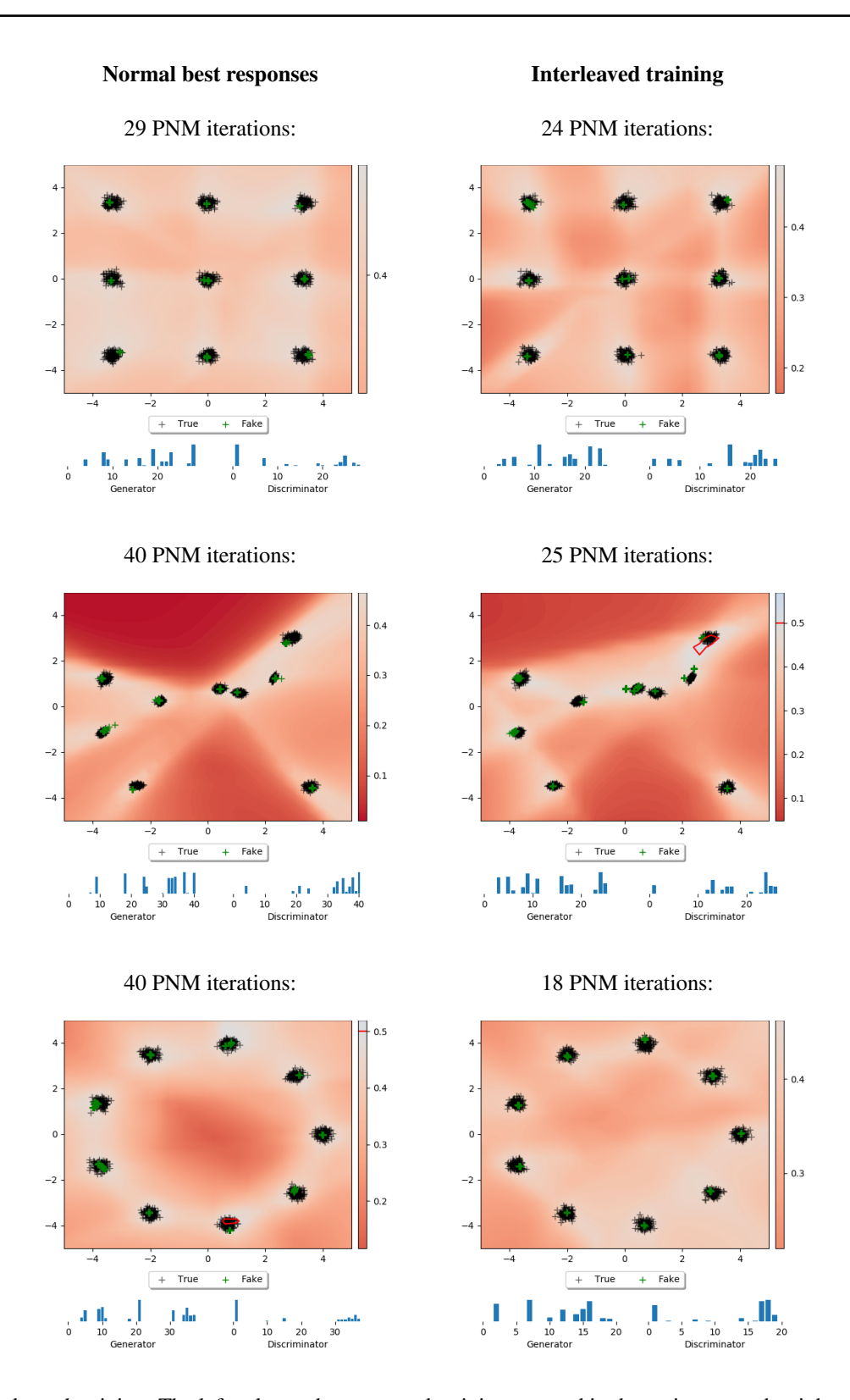


Figure 11: Interleaved training. The left column shows normal training, as used in the main paper; the right column shows interleaved training. In all cases, we manually picked the first iteration where all modes are covered. This consistently took less iterations for interleaved training, while solution quality was comparable.